International Journal of Nanomedicine

Dovepress
Taylor & Francis Group

Open Access Full Text Article

ORIGINAL RESEARCH

Aloe Vera Gel and Rind-Derived Nanoparticles Mitigate Skin Photoaging via Activation of Nrf2/ARE Pathway

Zixuan Sun[1,2,*], Yuzhou Zheng[2,*], Tangrong Wang[2,*], Jiaxin Zhang[2], Jiali Li[2], Zhijing Wu[2], Fan Zhang[2], Tingxin Gao[2], Li Yu[2], XueZhong Xu[1], Hui Qian[2], Yulin Tan[1]

[1]Department of General Surgery, Wujin Hospital Affiliated with Jiangsu University, Changzhou, 213017, People's Republic of China; [2]Jiangsu Key Laboratory of Medical Science and Laboratory Medicine, Department of Laboratory Medicine, School of Medicine, Jiangsu University, Zhenjiang, 212013, People's Republic of China

*These authors contributed equally to this work

Correspondence: Hui Qian, Jiangsu Key Laboratory of Medical Science and Laboratory Medicine, Department of Laboratory Medicine, School of Medicine, Jiangsu University, Zhenjiang, 212013, People's Republic of China, Email lstmmmlst@163.com; Yulin Tan, Department of General Surgery, Wujin Hospital Affiliated with Jiangsu University, Changzhou, 213017, People's Republic of China, Email tanyulin@wjrmyy.cn

Background: Skin aging is the primary external manifestation of human aging, and long-term exposure to ultraviolet radiation is the leading cause of photoaging, which can lead to actinic keratosis and skin cancer in severe cases. Traditional treatments may pose safety risks and cause side effects. As an emerging research direction, plant-derived exosome-like nanoparticles (PDNPs) show promise in combating aging. *Aloe vera*, known for its natural active ingredients that benefit the skin, aloe-derived exosome-like nanoparticles (ADNPs) have not yet been studied for their potential in delaying skin aging.

Methods: In this study, nanoparticles were isolated from two different sites, *aloe vera* gel and *aloe vera* rind (gADNPs and rADNPs), and characterized by TEM, SEM, AFM, NTA and BCA. The effects were evaluated by constructing in vitro and in vivo models and using RT-qPCR, immunofluorescence, and histopathological analysis.

Results: The results first revealed the exceptional anti-aging effects of ADNPs. We found that ADNPs promoted the nuclear translocation of Nrf2, alleviated oxidative stress and DNA damage induced by UV exposure, and inhibited the elevation of β-gal and SASP. In vivo, ADNPs reduced MDA and SOD levels in mouse skin tissue and delayed skin photoaging. Moreover, safety assessments confirmed the excellent biocompatibility of ADNPs.

Conclusion: ADNPs delay skin photoaging through the Nrf2/ARE pathway, holding potential clinical application value, and may provide new therapeutic strategies for future medical cosmetology and skin disease prevention.

Keywords: *aloe vera*, anti-aging, nanoparticles, skin photoaging, cellular senescence, antioxidants

Introduction

The skin serves as the body's primary defense, safeguarding it against external physical and chemical agents as well as diverse microbes but is also the most vulnerable to the influence of the external environment, leading to damage or aging parts. Ultraviolet radiation produced by solar radiation causes nearly 80% of skin aging, which is called skin photoaging.[1,2] Ultraviolet radiation (UV) is categorized into three types based on wavelength: UVA long-wave (320–400 nm), UVB medium-wave (280–20 nm), and UVC short-wave (100–280 nm),[3] of which UVC is completely absorbed and blocked before it reaches the atmosphere, and therefore photoaging due to ultraviolet radiation can be regarded as the effect of UVA (95%) and UVB (5%). Depending on its wavelength and energy, UVB energy is prone to cause apoptosis and DNA damage of skin cells, as well as inflammatory reactions such as redness and blistering. UVA is considered to be the main culprit of photoaging due to its long wavelength, which can profoundly infiltrate the dermis and induce the activation of MMP1, resulting in accelerated skin aging.[4–6] Clinical manifestations of photoaging include roughness,

Received: 19 December 2024
Accepted: 21 March 2025
Published: 2 April 2025

Graphical Abstract

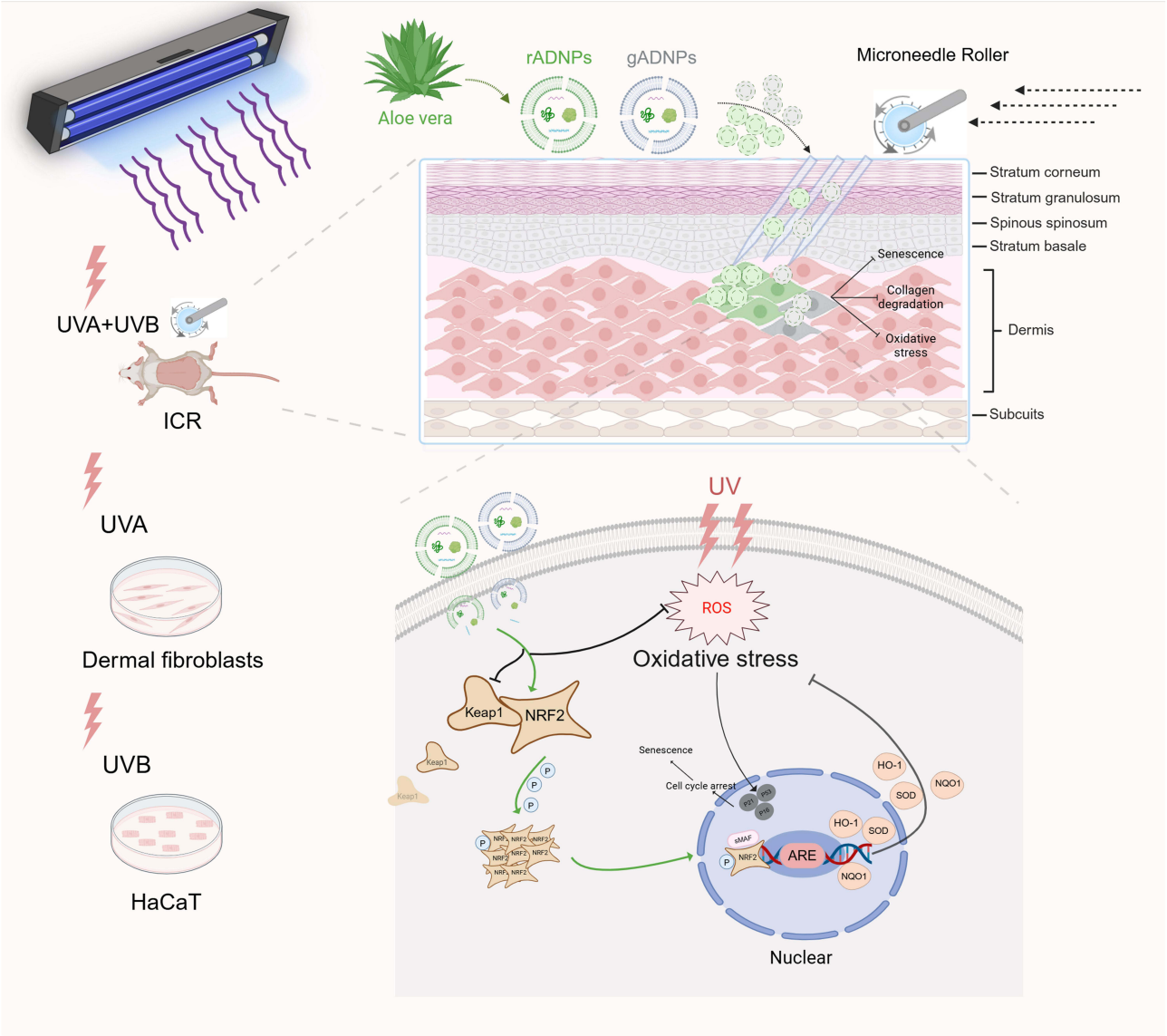

thickening and dryness of the irradiated parts of the skin, skin laxity, deepening and thickening of wrinkles, and even various benign or malignant tumors, freckle-like nevus (69.5%), actinic keratosis (22.3%), basal cell carcinoma (5.07%), melanoma (0.54%), and squamous cell carcinoma (0.36%) may appear.[7–10] This has brought a tremendous burden on individuals, families and society, therefore, identifying therapies that can alleviate photoaging is crucial for the advancement of pharmaceuticals and skincare products.

In recent years, the development of nanoformulations including liposomes, polymer nanoparticles, nanoemulsions, and nanofibers has provided more options for skin diseases. For example, nanofibers prepared by electrospinning technology carry natural active ingredients to combat photoaging by inhibiting the expression levels of aging genes in skin cells after UV irradiation.[11] With their unique size effect (<1000 nm), high specific surface area and tunable physicochemical properties, the transdermal efficiency of active ingredients is significantly enhanced, however, the accumulation risk and stability of such artificial nanofibers need to be deeply explored.[12] Plant-derived exosome-like nanoparticles (PDNPs), as one of the emerging research directions, have also shown great potential in the application of

dermatological system-related diseases.[13] For example, Tu et al[14] successfully isolated exosome-like nanoparticles (DDNPs) from Dendrobium and found that they were able to significantly contribute to accelerated healing of cutaneous wounds in mice by inhibiting the overexpression of IL-1β. Potato exosomes (ExoPs) were shown to have the ability to penetrate keratinocyte (HaCaT) and to inhibit the expression of collagen degrading enzymes (MMP1, 2, 9) and inflammatory cytokines (IL6, TNF-α) to reverse UVB radiation damage.[15] These findings underscore the potential use of plant-derived nanoparticles as a natural, reliable, and efficient therapeutic tool in the field of skin, while PDNPs present a reduced immunological risk and exhibit fewer side effects compared to mammalian-derived exosomes,[16] hence mitigating apprehensions regarding possible animal or human diseases.

Aloe vera is a miraculous gift of nature, known as "universal medicine", "natural beautician". The genus has about 550 species and the leaves and roots of *aloe vera* contain a variety of rich phytochemical pharmacological active ingredients, including aloe-emodin, aloin, β-sitosterol, quercetin, flavonoids, anthraquinones and a variety of phenolic compounds,[17,18] which are widely used as food and herbal medicine in the world. The genus *aloe vera* has been known for its proven medicinal properties of antioxidant, anti-inflammatory, antimicrobial and anticarcinogenic effects, and is particularly relevant to the fields of skin disorders, medical aesthetics and damage repair.[19–22] Wahedi et al[23] found that aloin accelerates skin wound healing and promotes cell migration and angiogenesis via regulating MAPK/Rho and Smad signaling pathways. Rodrigues et al[24] demonstrated that *aloe vera* extract enhanced lysosomal stability to protect cells from UVA-induced photodamage. These studies suggest that *aloe vera* and its active ingredients have great potential in resisting UV damage and delaying skin aging. While aloe-derived exosome-like nanoparticles (ADNPs), as carriers of aloe's natural active ingredients, not only possess the potential of plant nanoparticles, such as low immunogenicity, low cost, and ease of industrialization, but also feature characteristics like the ability to cross biological barriers, efficient intercellular communication, and tunability, which hold great promise for future translational applications in medical cosmetology and the prevention and treatment of clinical skin diseases.

Currently, there are very limited studies related to nanoparticles derived from *aloe vera*, with only a few mainly focusing on isolation attempts, anti-inflammatory, antioxidant, and wound healing as themes.[25–29] It is worth mentioning that Zeng et al[30] encapsulated the ICG into *aloe vera* gel-derived nanoparticles (gADNPs) and found that they could damage melanoma cells and inhibit tumor growth, which verified that ADNPs have good drug delivery ability and skin permeability. However, there has been no research on ADNPs in the field of anti-skin aging. Therefore, in this paper, we isolated and extracted aloe gel and rind-derived nanoparticles (gADNPs and rADNPs). We comprehensively evaluated their anti-skin photoaging ability for the first time in vivo and in vitro models and investigated their possible mechanisms of action. The aim is to provide new interventions for the development of cost-effective and safe anti-aging treatments for the skin, while also laying the groundwork for exploring other plant-derived nanoparticles for therapeutic and drug delivery.

Materials and Methods

Isolation of gADNPs and rADNPs

Wash fresh *aloe vera*, and separate the gel and rind. Mix the gel or rind, phosphate buffer saline (PBS, Meilunbio), and PBS ice in a certain weight ratio and extract the juice with a wall-breaker, while pectinase can be optionally added to achieve a mass fraction of 0.5%. After filtering through a 100-mesh strainer to remove residues, *aloe vera* gel or *aloe vera* rind mixture is obtained. The two mixtures underwent successive centrifugation at 300–350×g, 1000×g, 3000×g, and 11,000×g, respectively. Subsequently, it was ultracentrifuged at 150,000×g twice. The final precipitate was collected and resuspended in PBS to obtain aloe exosome-like nanoparticles.

Identification and Tracking of gADNPs and rADNPs

The nanoparticle tracking analysis (NTA, Particle Metrix) was applied to detect the particle size and concentration of gADNPs and rADNPs. The morphology, size, and profile of gADNPs and rADNPs were examined using transmission electron microscopy (TEM, FEI Tecnai 12, Philips), atomic force microscopy (ATM, Shimadzu SPM-9700), and scanning electron microscopy (SEM, Regulus 8100). The protein concentration of gADNPs and rADNPs was quantified by BCA protein assay kit (Vazyme). In vivo, the dorsal skin of mice was treated with DiR (UElandy)-labeled gADNPs

and rADNPs in conjunction with a microneedle roller, and fluorescence was detected using a small animal live imager (Pearl Imager, LI-COR). In vitro, uptake of Dil (Invitrogen)-labeled gADNPs and rADNPs was visualized under a laser confocal microscope (Leica).

Cell Culture

Tissue blocks isolated from the dorsal skin of neonatal Sprague Dawley rats were used and cultured in α-MEM medium (Gbico) supplemented with 10% FBS (Vazyme), waiting for dermal fibroblasts (DFs) to crawl out and identify them, with the same conditions for subsequent cultures. HaCaT cells were cultured using DMEM medium (Pricella) and the rest of the conditions were the same. Animals purchased from the Experimental Animal Center of Jiangsu University (SCXK(SU) 2023-0017). The use of the DFs cells had ethical and institutional review board approval (UJS IACUC), and the HaCaT cell lines were purchased from Yu Chi (Shanghai) Biotechnology Co., Ltd. and characterized using short tandem repeat (STR) analysis.

Western Blot

Total protein from cells was separated by SDS-PAGE and transferred to PVDF membranes (Millipore). Membranes were blocked with 5% skim milk in TBST for 2 hours, followed by overnight incubation with primary antibodies at 4°C, the dilution was prepared according to the instructions. After washing with TBST, membranes were incubated with HRP-conjugated secondary antibody (Invitrogen) for 2 hours. After further washing, proteins were detected using ECL (Vazyme) and visualized with a chemiluminescence gel imager (e-BLOT).

UV-Irradiation Photoaging Model and Treatment

The animal experiment was approved by the Institutional Animal Care and Use Committee of Jiangsu University (UJS IACUC). The serial number is UJS-IACUC-2024070202. Thirty-six female ICR mice (23 ± 2 g, 7 weeks old) were used for in vivo experiments (purchased from the Experimental Animal Center of Jiangsu University, SCXK(SU) 2023-0017) and kept at 22 ± 2°C with sufficient food and water (12 hours light/dark cycle) (SYXK(SU) 2023-0081). The feed was acclimatized for one week before the formal experiment, and then randomly divided into 6 groups of 6 animals each: control group (CTR), UV irradiation group (UV), UV + microneedle roller group (MN), UV + microneedle roller + PBS group (PBS), UV + microneedle roller + gADNPs group (gADNPs), and UV + microneedle roller + rADNPs group (rADNPs). Except for the CTR group, each group was irradiated with UVA+UVB for 4 cycles. On day 1 of each cycle, animals in the MN group were treated with microneedle rollers, and animals in the last 3 groups were treated with microneedle rollers and counterparts. The light dose was 1 MED in the first round, which was increased to 1.5 MED in the second round, and 2 MED in the third and fourth rounds. The light dose was determined based on the results of the preexperiment.

In vitro, DFs/HaCaT were inoculated into six-well plates (ExCell) and pretreated with gADNPs and rADNPs for 24 hours. DFs/HaCaT were irradiated under 365 nm UVA lamp (Philips, Shanghai, China) / 311 nm UVB lamp (Philips, Shanghai, China).

Cell Viability

1×10^3 DFs/HaCaT were inoculated in 96-well plates (ExCell), and following UVA/UVB irradiation. CCK8 (Vazyme) was introduced to each well and co-cultured with cells for 2 hours in darkness. The OD at 450 nm was subsequently measured using a microplate reader (Bio Tek).

RT-qPCR

Total RNA was extracted using Trizol reagent (Invitrogen). The cDNA synthesis was conducted via a reverse transcription kit (Vazyme). RT-qPCR was performed in 96-well plates using AceQ qPCR SYBR green master mix (Vazyme). All primers used in this study were synthesized by Sangon Biotech, with their sequences are provided in Supplementary Table S1.

SA-β-Gal Staining Analysis

Using the SA-β-gal Staining Kit (Yeasen Biotechnology, Shanghai), the cells were firstly fixed with fixative for 15 minutes at room temperature. Subsequently, the staining solution was added and incubated overnight at 37°C in an incubator devoid of CO_2. The result was observed by microscope (Nikon) the next day.

Immunofluorescence Staining

Cells or tissue sections were fixed with 4% paraformaldehyde, permeabilized with 0.1% Triton X-100, and blocked with 5% BSA. Samples were incubated with primary antibody overnight at 4°C, followed by incubation with fluorophore-conjugated secondary antibody Alexa Fluor™ 555 (Invitrogen) for 1.5 hours at room temperature. After washing, nuclear staining was performed with Hoechst 33342 (Sigma Aldrich). Samples were imaged using a fluorescence microscope (Nikon).

Immunohistochemistry (IHC)

Paraffin sections of skin tissue were dewaxed and hydrated in xylene and each gradient of ethanol. The subsequent process was carried out according to the kit (Boster, SA1020), and at the end of the process, the sections were dehydrated and sealed using the opposite process.

Statistical Analysis

Statistical analyses were conducted using GraphPad Prism 9.0 software, with all data expressed as mean ± SD. Comparisons between two groups were made using an unpaired *t*-test, whereas one-way ANOVA was used for the assessment of multiple groups. P value<0.05 was considered statistically significant.

Results

Isolation and Characterization of gADNPs and rADNPs

Currently, most of the isolation methods for plant-derived nanoparticles are still ultracentrifugation (UC),[31,32] and we optimized the existing extraction protocol (Supplementary Figure 1A and B). We weighed and mixed the gel and rind, PBS buffer, and PBS ice cubes in a certain ratio by a wall breaker, filtered the sediment, and then subjected it to differential centrifugation and ultracentrifugation (Figure 1A and Supplementary Figure 2A). The gADNPs and rADNPs were assessed for size, shape, particle concentration, ζ-potential, and protein content. NTA indicated that the average particle concentrations of gADNPs and rADNPs were 5.3×10^{11} particles/mL and 4.1×10^{11} particles/mL, respectively, with average particle sizes of approximately 190 nm and 160 nm, respectively, and average ζ-potentials of −14.59 ± 0.68 and −24.26 ± 0.84 mV, respectively (Figure 1B and C). It was observed that both gADNPs and rADNPs had a typical oval or cup-shaped phospholipid bilayer structural morphology, as well as a smooth and flat surface with good dispersion and no large clusters (Figure 1D–G). The protein content of gADNPs was detected to be nearly three times that of rADNPs (Figure 1H), with a distribution in the range of 15–180 kDa (Figure 1I). In addition, we co-incubated the two nanoparticles with DFs in vitro, which showed no difference from the control group within 72 hours (Figure 1J). The above results indicated that we successfully extracted *aloe vera* gel and rind-derived nanoparticles and successfully validated their biosafety in vitro.

Protective Effects of gADNPs and rADNPs on UVB-Injured HaCaT Cells

Based on the fact that the epidermal layer in the skin is mainly damaged by UVB in ultraviolet light,[33] we established a model of UVB-induced acute photodamage to HaCaT cells. We found that DiO membrane dye-labeled gADNPs and rADNPs could be successfully taken up by HaCaT cells (Figure 2A). UVB irradiation of HaCaT cells with a dose of 80 mJ/cm^2 showed that HaCaT cells produced a large amount of ROS, while pretreatment with gADNPs and rADNPs significantly inhibited ROS production (Figure 2B). Immunofluorescence and RT-qPCR results indicated that the expression of TNF-α and TGF-β, significant indicators of inflammation, were elevated in HaCaT cells after UVB irradiation and down-regulated after gADNPs and rADNPs treatment (Figure 2C and D). The impaired migratory ability of HaCaT cells was restored and the proliferation level was increased compared with UVB group (Figure 2E and F),

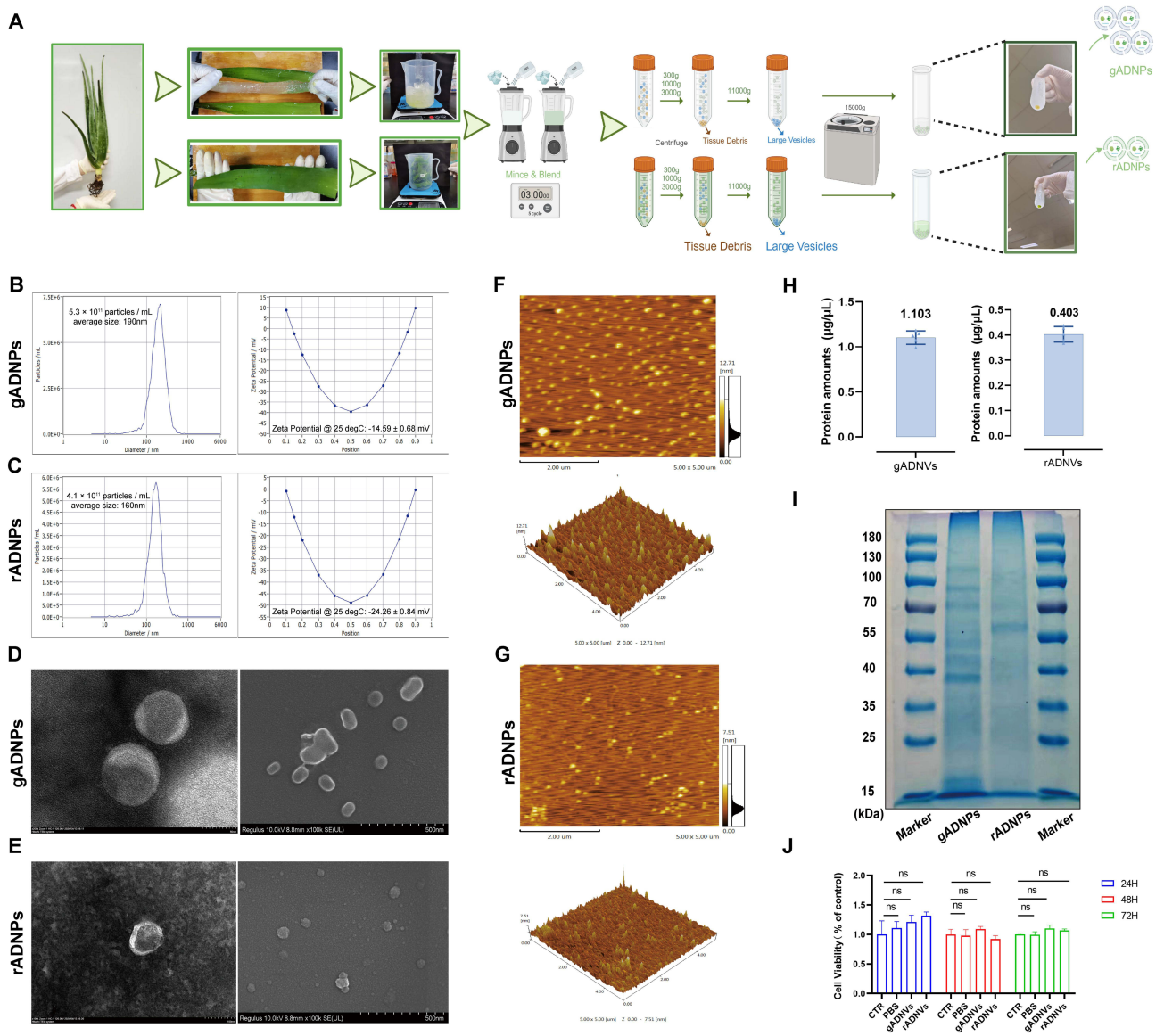

Figure 1 Isolation and Characterization of gADNPs and rADNPs. (**A**) Schematic diagram of the separation and extraction process of gADNPs and rADNPs. (**B**) NTA analysis of the size, concentration, and ζ potential of gADNPs. (**C**) NTA analysis of the size, concentration, and ζ potential of rADNPs. (**D**) TEM and SEM electron micrographs of gADNPs (scale bars are 50nm/100nm). (**E**) TEM and SEM electron micrographs of rADNPs (scale bars are 50nm/100nm). (**F**) AFM electron micrograph of gADNPs (scale bars are 2 μm). (**G**) AFM electron micrograph of rADNPs (scale bars are 2 μm). (**H**) Protein content of gADNPs and rADNPs measured using the BCA assay. (**I**) SDS-PAGE and Coomassie Brilliant Blue staining to analyze protein distribution in gADNPs and rADNPs. (**J**) In vitro safety evaluation using CCK8 after co-incubation of gADNPs and rADNPs with DFs.

Abbreviation: ns, no significant difference.

which was also confirmed by Western blot (Figure 2G). The above results confirm that gADNPs and rADNPs exert a protective effect on damaged HaCaT cells and help restore their normal function. UV radiation-induced inflammatory damage accelerates skin photoaging,[33] and we further investigated the function of gADNPs and rADNPs in UVA-induced photoaging of DFs.

Evaluation of gADNPs and rADNPs for Delayed Photoaging of DFs

We extracted and characterized primary DFs (Supplementary Figure 2B) and constructed a UVA-induced photoaging model. The results showed that DFs successfully uptook Dil-labeled gADNPs and rADNPs (Figure 3A). The proportion of cells carrying labeled fluorescent signals at 12 hours and 24 hours was examined by flow cytometry. The results showed that nearly half of the DFs successfully absorbed gADNPs and rADNPs at 12 hours, and nearly 80% of the cells

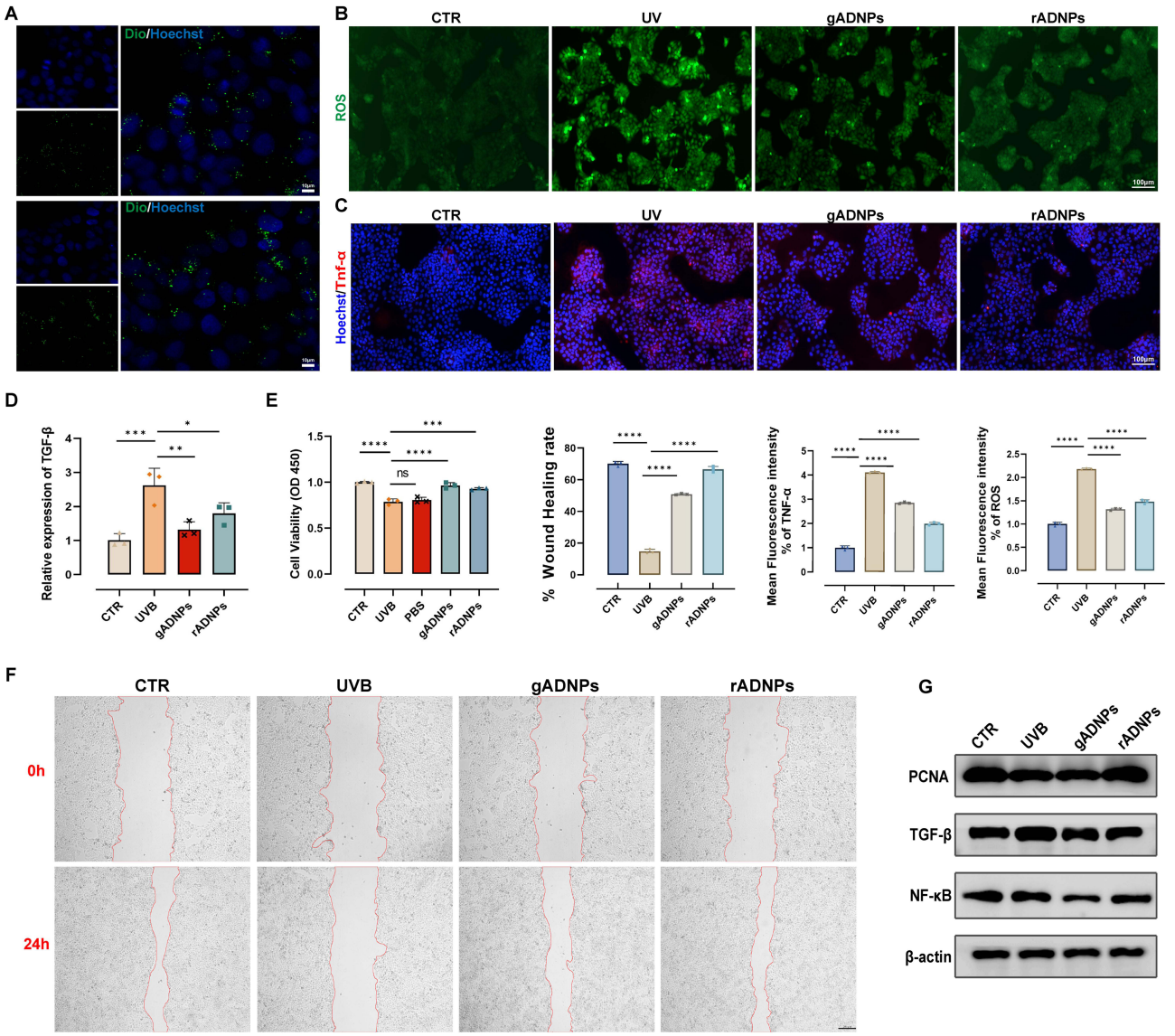

Figure 2 Protective effects of gADNPs and rADNPs on HaCaT cells. (**A**) Uptake of gADNPs and rADNPs by HaCaT cells (scale bars are 10 μm). (**B**) Detection of ROS levels after oxidative stress in HaCaT cells (scale bars are 100 μm). (**C**) Immunofluorescence detection of TNF-α expression level (scale bars are 100 μm). (**D**) RT-qPCR detection of TGF-β gene expression level. (**E**) CCK8 assay for the proliferation and viability of HaCaT cells after UVB irradiation. (**F**) HaCaT cells scratch assay (scale bars are 200 μm). (**G**) Western Blot detection of changes in PCNA, TGF-β, BCL-2, and NF-κB in HaCaT cells after UVB irradiation. Data are presented as mean ± SD. n = 3, *P < 0.05, **P < 0.01, ***P < 0.001, ****P < 0.0001.

Abbreviation: ns, no significant difference.

carried fluorescent signals after 24 hours (Figure 3B). It indicated that the uptake process of gADNPs and rADNPs by DFs was time-dependent, suggesting that the potential therapeutic effect was related to the treatment time. We then replicated the ability of gADNPs and rADNPs to restore migration and promote proliferation in DFs as validated in HaCaT cells and obtained approximate results (Supplementary Figure 3A and B). In addition, we increased the dose of UVA to induce apoptosis in DFs, and the proportion of DFs with early and late apoptosis in the gADNPs and rADNPs group was reduced by 22.16% and 15.48%, respectively (Figure 3C). Prolonged UV irradiation leads to sustained apoptosis, which may result in actinic keratosis, skin cancer, and atopic dermatitis in severe cases.[34,35] These results strongly support its potential application in anti-UV damage therapy or skincare products.

The generation and buildup of ROS result in DNA damage and cell cycle arrest, serving as a critical element in skin aging.[36,37] We observed that ROS expression levels in DFs were significantly elevated after UVA irradiation, and gADNPs and rADNPs pretreatment played different inhibitory roles (Figure 3D). The experiment was repeated by flow cytometry and

https://doi.org/10.2147/IJN.S510352

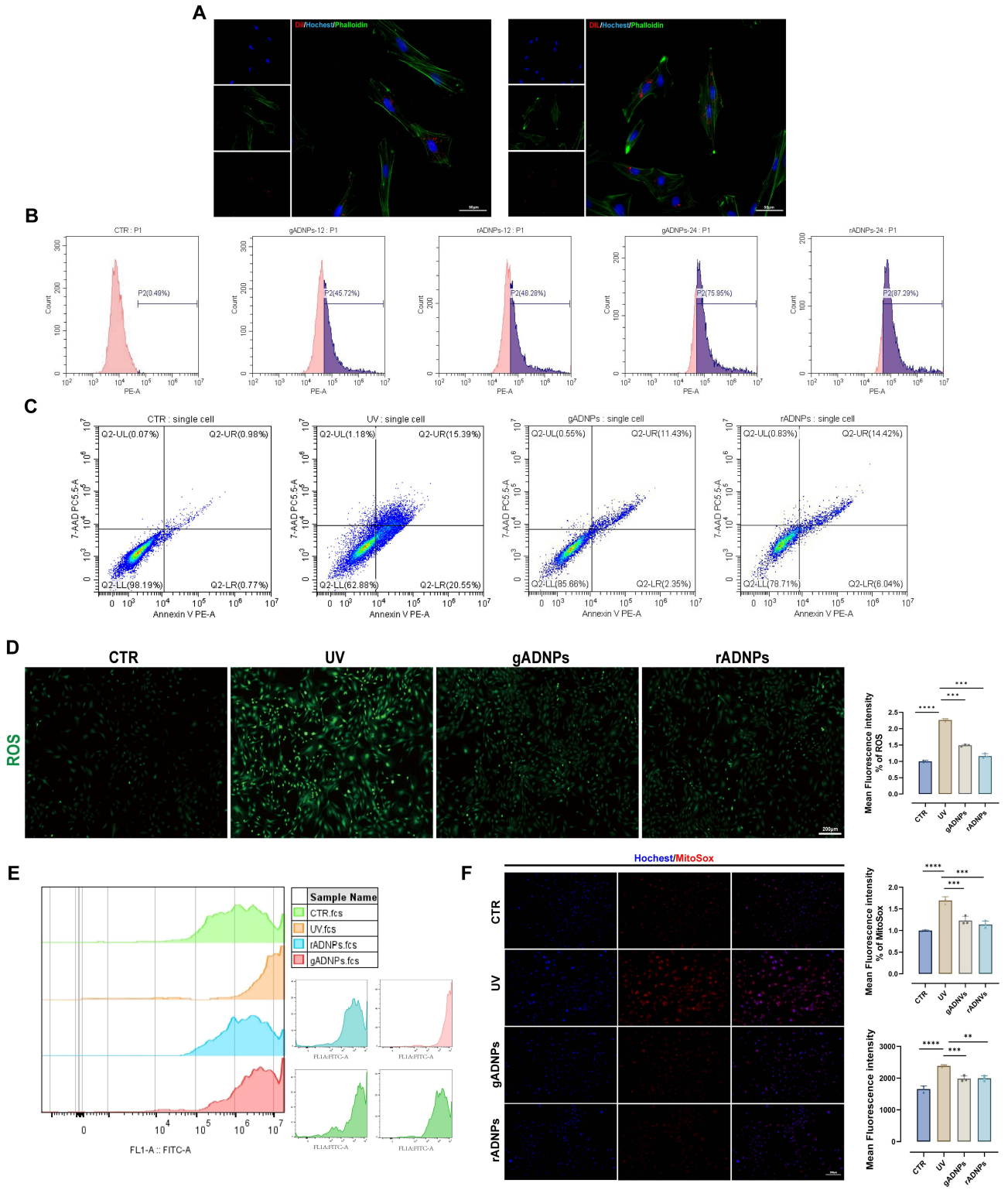

Figure 3 gADNPs and rADNPs restore DFs function and counteract UVA-induced oxidative stress. (**A**) Uptake of gADNPs and rADNPs by DFs (scale bars are 50 μm). (**B**) Flow cytometry analysis of gADNPs and rADNPs uptake by DFs at different time points. (**C**) Flow cytometry detection of apoptosis percentage in DFs after gADNPs and rADNPs treatment. (**D**) Images of ROS generation in DFs from different groups and their corresponding quantification (scale bars are 200 μm). (**E**) Flow cytometry analysis of ROS generation in DFs and their quantification maps (right panel). (**F**) Fluorescence images of mitochondrial ROS (MitoSoX probe) expression after gADNPs and rADNPs treatment and their quantification plots. Data are presented as mean ± SD. n = 3, **P < 0.01, ***P < 0.001, ****P < 0.0001.

Abbreviation: ns, no significant difference.

the same results were obtained (Figure 3E). In addition, mitochondrial ROS (MitoSoX probe) was effectively inhibited by gADNPs and rADNPs (Figure 3F), suggesting a reversal of mitochondrial dysfunction and a reduction in oxidative damage. This provides new opportunities to explore the mechanisms of action of gADNPs and rADNPs. We then founded that UVA exposure resulted in the down-regulation of the expression levels of COL1A1, a major structural protein of the ECM, and LaminB1, a nuclear fiber layer protein intimately associated with cellular senescence (Figure 4A). The cell cycle arrest-related markers P16, P53 and P21, the DNA damage markers γ-H2AX and 53BP1, and the typical SASPs IL-6 and CXCL1, were also elevated (Figure 4B and C). Excitingly, gADNPs and rADNPs pretreatment improved their expression by direct or indirect methods. Furthermore, SA-β-gal, a reliable marker for detecting cellular senescence,[38,39] showed that gADNPs and rADNPs pretreatment inhibited the production of SA-β-gal (Figure 4D). The above results suggest that *aloe vera* gel and rind-derived nanoparticles can alleviate photoaging of DFs.

gADNPs and rADNPs Protected Mice Against UV-Induced Skin Photoaging

Existing models of skin photoaging mainly use UVA or UVB irradiation alone.[40,41] In order to better simulate the UV component of sunlight, we developed an in vivo model of skin photoaging created through the combination of UVA and UVB in ICR mice (Figure 5A). ICR mice were randomly divided into six groups: CTR, UV, MN (UV+MN), PBS (UV +MN+PBS), gADNPs (UV+MN+gADNPs), and rADNPs (UV+MN+rADNPs).

To observe the absorption and metabolizability of gADNPs and rADNPs in mice, we applied Dil/DiR-labeled gADNPs and rADNPs to the skin via a microneedle roller and found that gADNPs and rADNPs could be delivered to the dermis (Supplementary Figure 4A). In vivo imaging showed that the delivered gADNPs and rADNPs were metabolized at an accelerated rate only after 72 hours (Supplementary Figure 4B), indicating that the nanoparticles could remain active and functional in the skin tissue for a period of time. Based on the results of the minimum erythemal dose (MED) assay (Supplementary Figure 4C),[42] finally, we set the irradiation dose for the first cycle at 1 MED. After irradiation, we compared the dorsal skin of ICR mice exposed to light (Figure 5B). Compared to the control group, the dorsal skin of UV-irradiated mice displayed typical photoaging phenotypes, including roughness, dryness, erythema, desquamation, and wrinkles. In contrast, the gADNPs and rADNPs groups showed varying degrees of improvement, with rADNPs appearing to be more effective than gADNPs. This observation is consistent with previous cellular studies, and we will explore the possible underlying mechanisms in the discussion.

Histological analysis was used to further elucidate the effect of gADNPs and rADNPs intervention. HE staining showed that mice subjected to UVA and UVB irradiation exhibited increased keratinization of the epidermal layer, thickening of acanthocytes, and varying degrees of inflammatory cell infiltration. Neither microneedle rollers alone nor microneedle roller-mediated PBS treatment was effective, whereas gADNPs and rADNPs showed significant improvement (Figure 5C). The rADNPs group exhibited the best phenotype, with an average epidermal thickness of 15.82 ± 6.75 μm, nearly approaching the normal group, compared to 88.45 ± 4.62 μm in the UV group. gADNPs and rADNPs increased the collagen volume fraction reduced by UV irradiation, with the rADNPs group showing an additional 3.5% increase (Figure 5D). EVG staining showed that the number of elastic fibers (black dots) was significantly reduced after UV irradiation, but the elastic fibers in both the gADNPs and rADNPs groups were restored to varying degrees (Figure 5E).

SASPs, such as TFG-β and IL-6, significantly influence the aging process.[38,43] Senescence is a state in which cells permanently stop proliferating and is usually triggered by cell cycle dysregulation, in which P53 plays an important role. Tissue immunofluorescence and RT-qPCR showed that gADNPs and rADNPs effectively attenuated the elevation of P53, P21, TGF-β and IL-6 expression after UV irradiation, and protected skin structure and function (Figure 6A and B). Meanwhile, MDA and SOD levels were measured in the skin tissues of irradiated mice. Results showed increased MDA expression and significantly reduced SOD activity in the model group. However, gADNPs and rADNPs treatment alleviated oxidative stress in skin tissues (Figure 6C and D). By immunohistochemical staining, we found that 8-OHdG and MMP1 were elevated and type I collagen and PCNA were decreased after UV irradiation, which were improved in the gADNPs and rADNPs treatment group (Figure 6E). In conclusion, these results suggested that treatment with gADNPs/rADNPs was effective in alleviating UV-induced skin photoaging in mice.

The in vivo biosafety of nanomedicines is a prerequisite for their medical translation. Serum indices of liver and kidney functions were examined in mice and showed no difference in changes (Supplementary Figure 5A). In addition, no pathological alterations were seen in the principal organs of the mice (Supplementary Figure 5B), and the weight

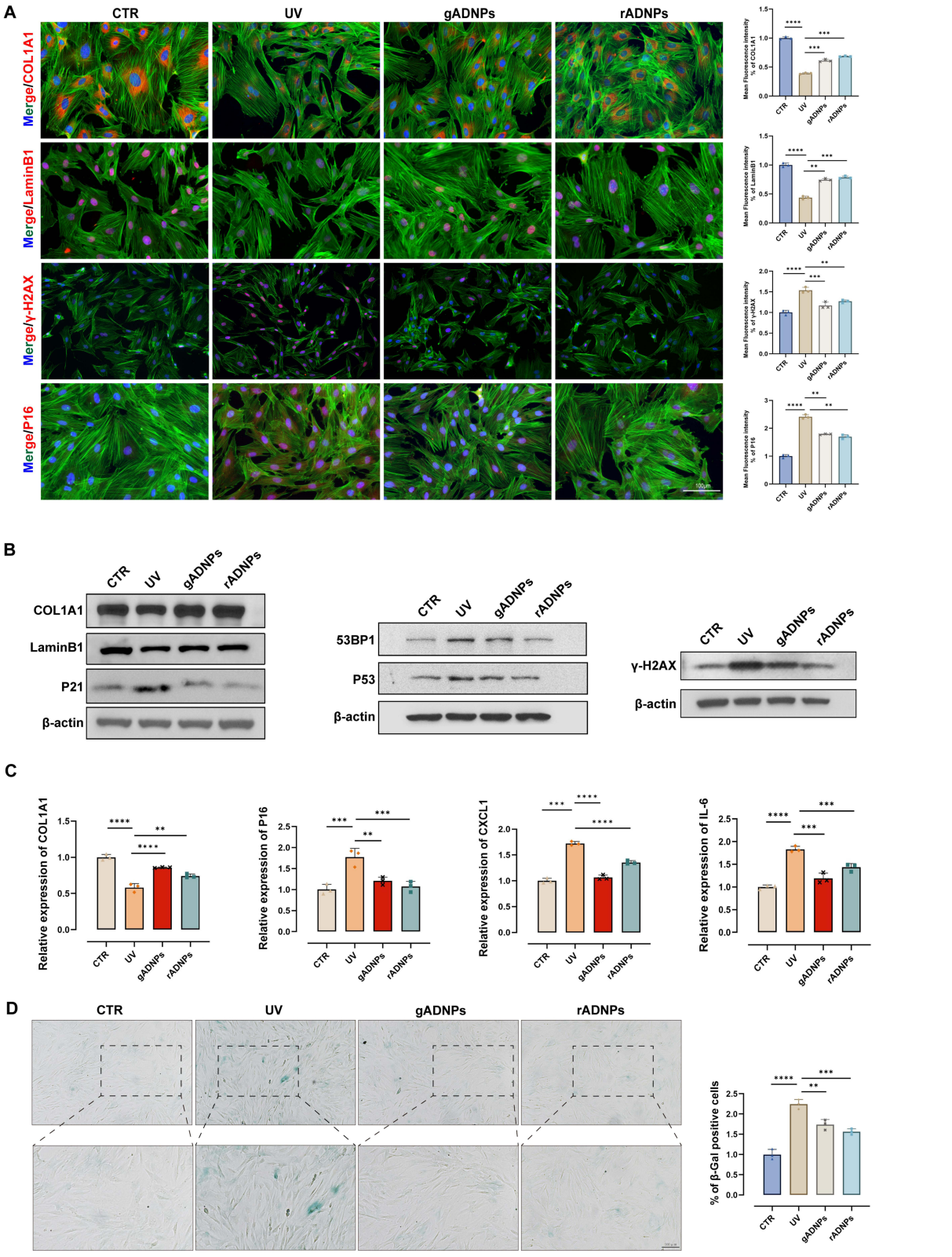

Figure 4 gADNPs and rADNPs inhibit SASP generation and restore senescence-associated cell cycle arrest. (**A**) Immunofluorescence detection of COL1A1, LaminB1, γ-H2AX, and P16 expression changes in DFs after UVA-induced treatment with gADNPs and rADNPs (scale bars are 100 μm). (**B**) Western blot analysis of senescence-related markers (P21, P53, LaminB1) and DNA damage markers (γ-H2AX, 53BP1) in DFs after gADNPs and rADNPs treatment. (**C**) RT-qPCR detection of COL1A1, P16, CXCL1, and IL-6 gene expression changes after gADNPs and rADNPs treatment. (**D**) Representative images of SA-β-gal staining in DFs (scale bars are 100 μm). Data are presented as mean ± SD. n = 3, **P < 0.01, ***P < 0.001, ****P < 0.0001.

Abbreviation: ns, no significant difference.

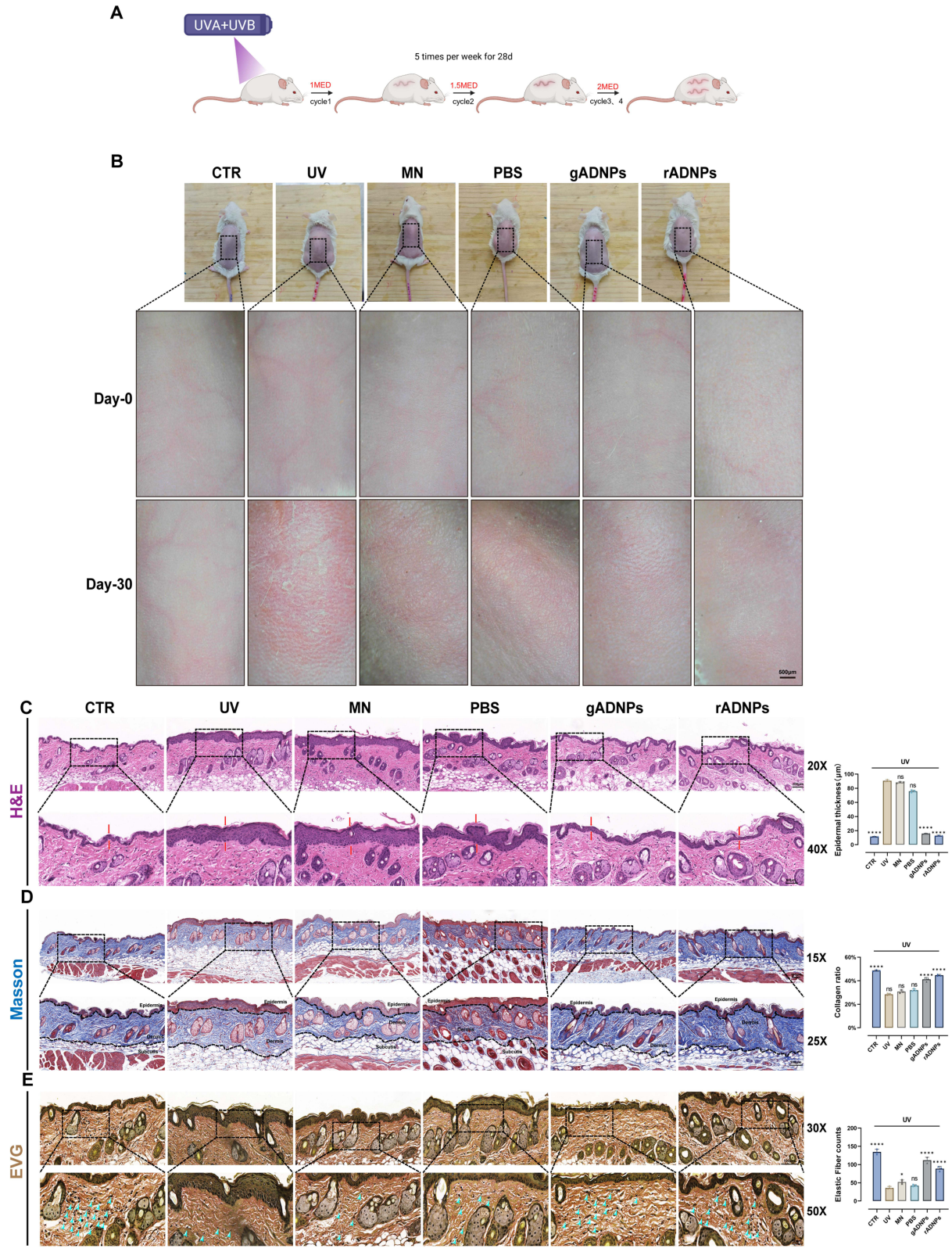

Figure 5 Pathologic analysis of skin tissues in mice treated with gADNPs and rADNPs. (**A**) Schematic diagram of the in vivo photoaging model using UVA and UVB combined irradiation. (**B**) Gross phenotype of mouse skin in each group after UV irradiation. (**C**) Representative images of H&E staining of mice after 4 weeks of treatment (Scale bars are 50 μm in full view, 20 μm in magnified view). (**D**) Representative images of Masson staining of mice after 4 weeks of treatment (Scale bars are 100 μm in full view, 50 μm in magnified view). (**E**) Representative images of EVG staining of mice after 4 weeks of treatment (Scale bars are 50 μm in full view, 20 μm in magnified view, blue arrow points to the elastic fibers). Data are presented as mean ± SD. n = 3, **P < 0.01, ***P < 0.001, ****P < 0.0001.
Abbreviation: ns, no significant difference.

https://doi.org/10.2147/IJN.S510352

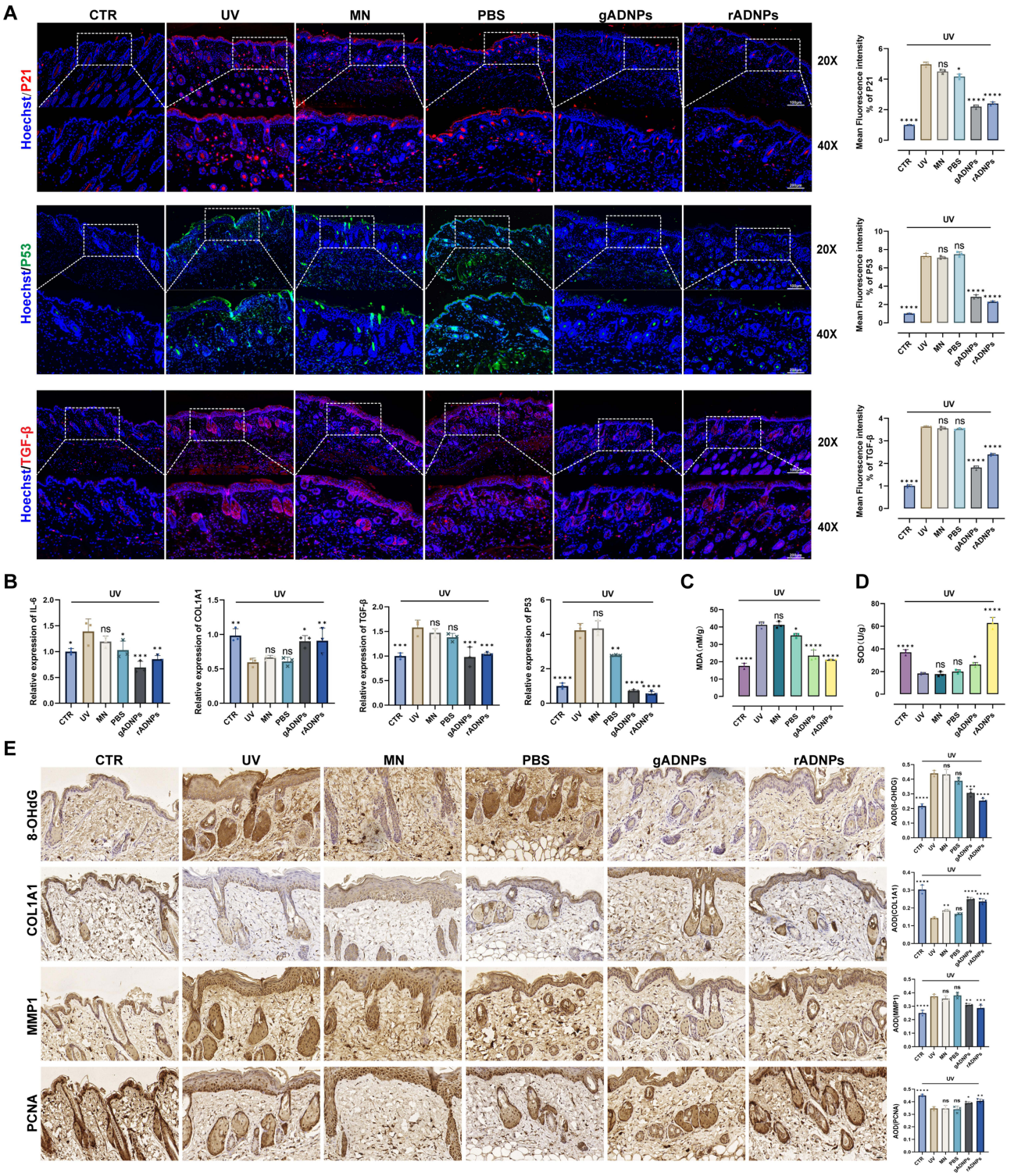

Figure 6 Immunofluorescence and immunohistochemical staining analysis of skin tissue. (**A**) Immunofluorescence (IF) images of mouse skin labeled with P53, P21, and TGF-β (Scale bars are 100 μm for full view, 200 μm for magnified view). (**B**) RT-qPCR analysis of gene expression in mouse skin tissue. (**C** and **D**) Relative MDA and SOD activity levels in the dorsal skin of mice after 4 cycles of treatment. (**E**) Representative images of immunohistochemical staining of mouse skin (Scale bars are 20 μm). Data are presented as mean ± SD. n = 3, *P < 0.05, **P < 0.01, ***P < 0.001, ****P < 0.0001.

Abbreviation: ns, no significant difference.

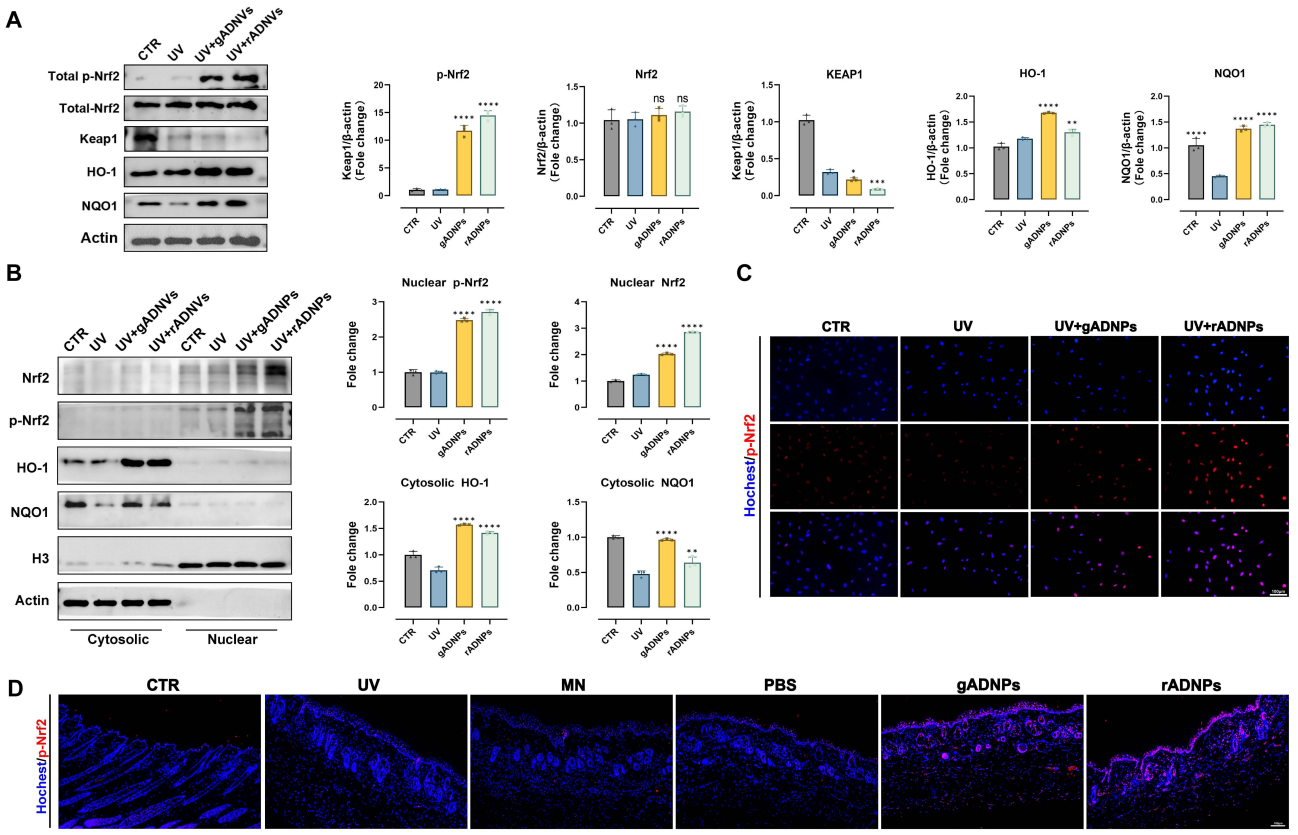

Figure 7 Activation of NRF2 and its downstream antioxidant enzyme activities by gADNPs and rADNPs. (**A** and **B**) Western blot analysis of p-Nrf2, Nrf2, Keap1, HO-1 and NQO1 protein levels before and after gADNPs and rADNPs treatment. (**C** and **D**) Nuclear translocation expression of Nrf2 observed by IF staining of cells and tissues. Data are presented as mean ± SD. n = 3, *P < 0.05, **P < 0.01, ***P < 0.001, ****P < 0.0001.
Abbreviation: ns, no significant difference.

changes of mice in all groups fluctuated within a reasonable range during the experimental period (Supplementary Figure 5C), demonstrating that the in vitro and in vivo application of gADNPs and rADNPs has a favorable biosafety.

gADNPs and rADNPs Promote the Activation of the NRF2 Pathway

Nrf2 regulates the skin's antioxidant defense against environmental stimuli primarily by controlling the expression of the ARE gene.[44,45] ARE is a cis-acting element situated in the promoter region of Phase II detoxification enzymes. In reaction to oxidative stress and toxic stimuli, activated Nrf2 dissociates from Keap1, translocates to the nucleus, and binds to the ARE, therefore triggering the expression of antioxidant genes such as HO-1, NQO-1, and SOD,[46] which reduces the level of ROS and neutralizes oxidative stress in a deacetylase-dependent manner.[47] A variety of phytochemicals have been identified to target the Nrf2 pathway.[48] Our results showed that the differences in Nrf2 expression among the groups after UV irradiation were not significant. However, interestingly, treatment with gADNPs and rADNPs suppressed the expression of Keap1 and significantly promoted the expression level of phosphorylated Nrf2 as well as the downstream expression levels of NQO1 and HO-1 (Figure 7A). On this basis, we isolated nuclear and cytoplasmic proteins and showed that phosphorylated-Nrf2 was mainly expressed in the nucleus, whereas the gADNPs and rADNPs group significantly up-regulated the levels of HO-1 and NQO1 in the cytoplasm (Figure 7B). In addition, cell and tissue immunofluorescence results further verified the nuclear translocation expression of Nrf2 (Figure 7C and D), indicating that gADNPs and rADNPs can mitigate UV-induced skin photoaging via activating the Nrf2/ARE pathway.

Discussion

The rapid development of modern industrialization is damaging the ozone layer, leading to an increase in UV reaching the Earth's surface,[49,50] which causes skin damage and accelerated aging, and may also result in actinic keratosis and skin

cancer. Therefore, preventive measures for skin aging have gradually attracted increasing attention. Compared to traditional chemical therapies and physical treatments, the application of nanomedicine in the skin system has shown superior performance. For instance, the transdermal delivery efficiency of vitamin C was enhanced by 2.1 times when encapsulated in nanoscale liposomes.[51] However, synthetic nanocarriers may cause adverse reactions due to their irritant properties. Therefore, many researchers have turned to extracellular vesicles (EVs) mammalian (such as hair follicles, umbilical cord, and adipose tissue) to address this issue. EVs ranging from 30 to 150 nm, as a promising therapeutic strategy, participate in disease onset and progression by mediating intercellular communication. They have been applied in the treatment of various diseases. Photoaging is no exception; for instance, hucMSC-sEV have been shown to suppress inflammatory responses and improve skin hydration, thereby preventing photoaging.[6] Unfortunately, concerns about immune responses triggered by EVs and the potential pathogens they may carry still persist. In contrast, PDNPs effectively address these shortcomings of nanomedicines, which are becoming increasingly popular due to their high permeability, excellent biocompatibility, extremely low immunogenicity, and growing potential for large-scale applications. Based on this, we have focused our attention on *aloe vera*, which is closely related to the skin system, hoping to harness the natural power of ADNPs to address the challenges posed by photoaging.

This study provides substantial evidence supporting the therapeutic effects of ADNPs. First, we isolated nanoparticles (gADNPs and rADNPs) from *aloe vera* gel and rind, confirming the conclusion previously suggested by Ramirez et al[25] that ADNPs can promote migration and enhance cell viability. Subsequently, based on the different roles of UVA and UVB in the process of photoaging, we established HaCaT cell photodamage models and DFs cell photoaging models. We successfully demonstrated that ADNPs possess the ability to scavenge ROS generated by UVA and UVB exposure, protect DFs from DNA damage induced by UV irradiation, and reduce the formation of the aging marker β-gal. In vivo, ADNPs also alleviate skin photoaging in mice by inhibiting the elevation of aging markers P53, P21, and SASP, regulating the expression of MDA and SOD in skin tissues after UVA and UVB exposure, and reducing the level of oxidative stress. Finally, our results show that ADNPs can promote the nuclear translocation of Nrf2, increasing the synthesis of antioxidant genes to combat DFs photoaging.

The viscosity of *aloe vera* gel and rind extract has a significant impact on the concentration of the extracted ADNPs.[30] Therefore, based on the methods described by Ramirez et al[25] and Choi et al,[26] we added PBS ice cubes and pectinase, and increased the ultracentrifugation speed to 150,000×g in order to reduce the heat generated by mechanical forces during the process, which could damage the vesicles, while maintaining a low-temperature environment.[52] Under the same conditions, comparison of the results revealed that the concentrations of gADNPs and rADNPs were increased by at least 2- and 3-fold, respectively. Additionally, characterization results showed significant differences between gADNPs and rADNPs in terms of size, concentration, zeta potential, and protein content. These findings confirm that the extracted gADNPs and rADNPs are two distinct types of nanoparticles, and also indicate that even minor changes can affect the characterization results of PDNPs. In other words, we believe that even when sourced from the same plant, PDNPs isolated under different preparation protocols, pre-treatment conditions, growth environments, or from different plant parts will exhibit varying characteristics, and their composition will change accordingly. For example, in a study isolating PDNPs from sunflower and Arabidopsis, a simple change in centrifugation speed was found to cause significant differences in the contents of the extracted PDNPs.[53] Therefore, we urge the prompt establishment of standardized isolation protocols for PDNPs and the formulation of unified operating guidelines to ensure the comparability of results across different laboratories.

In addition, we found that the rind of aloe, often considered a waste byproduct in aloe applications, seems to have significant medicinal value in the field of tissue repair. Initially, we planned to use rADNPs as a control group for gADNPs. However, we discovered that rADNPs also possess anti-photoaging effects, and even outperform gADNPs in terms of anti-DNA damage and oxidative stress inhibition. This led us to realize that gADNPs and rADNPs exert the same effects through two distinct mechanisms. PDNPs are rich in various homologous substances derived from the parent plant. In contrast to the abundant soluble proteins and polysaccharides in *aloe vera* gel, the *aloe vera* rind contains anthraquinones, including aloenin A, aloenin B, aloin, and aloe-emodin,[18,54,55] the two derived nanoparticles differ in terms of their content and mechanisms of action in anti-photoaging pathways. The content analysis of ADNPs by Zeng

et al[30] and Ramirez et al[25] validated this point, showing that aloe-emodin, aloenin, and quercetin are more abundant in the *aloe vera* rind, while β-sitosterol, aloe polysaccharides, and β-glucan are present in higher concentrations in the gel.

Analogues of the 14-3-3ζ protein family were also found in ADNPs, Wu et al[56] confirmed that huMSC-sEVs activate the SIRT1 pathway by delivering 14-3-3ζ, thereby alleviating photodamage. Therefore, we hypothesize that gADNPs may repair the skin barrier, combat oxidative stress, and delay skin aging by providing similar 14-3-3ζ proteins or acetylated mannoglucans. In contrast, rADNPs may delay skin aging by inhibiting pathways associated with ROS generation through the enrichment of various antioxidant enzymes and anthraquinones. Our study focuses on evaluating the effects of ADNPs in alleviating oxidative stress and counteracting photoaging. However, the other mechanisms by which ADNPs mitigate photoaging remain to be further explored, in order to reveal additional novel targets of plant-derived nanoparticles in anti-aging research. For example, our results suggest that ADNPs are capable of inhibiting mitochondrial ROS production, indicating a restoration of mitochondrial dysfunction and respiratory chain efficiency. In recent years, the role of mitophagy in aging has received increasing attention, and how ADNPs promote mitophagy to combat aging warrants further investigation.[57]

According to the National Institutes of Health (NIH) statistics of clinical tests currently being recruited or in trials, there are currently no clinical trials involving PDNPs for skin aging. Although challenges such as technology, cost, and stability may arise, we still have strong reasons to believe that ADNPs have significant application potential in the prevention and treatment of clinical skin diseases, the field of medical aesthetics, and the cosmetics market.

Conclusion

In summary, this study successfully extracted nanoparticles with potential anti-photoaging properties from *aloe vera* gel and rind, providing substantial evidence to support this conclusion. In both in vivo and in vitro models, the two types of nanoparticles demonstrated excellent biocompatibility and the ability to delay skin photoaging. These effects are mediated through the activation of the Nrf2/ARE pathway to combat oxidative stress. Additionally, we found that aloe rind-derived nanoparticles, traditionally considered a byproduct, also exhibited unexpectedly significant effects. This study lays a theoretical foundation for the development of natural and safe anti-photoaging formulations, which are expected to hold considerable potential in the fields of functional skincare products and dermatology in the future.

Ethics Approval and Consent to Participate

The animal experiment was approved by the Institutional Animal Care and Use Committee of Jiangsu University (UJS IACUC). The serial number is UJS-IACUC-2024070202. All procedures in the manuscript were reviewed in advance by UJS IACUC and also met the guidelines of the National Institutes of Health Guide for the Care and Use of Laboratory Animals.

Acknowledgments

We are profoundly grateful to Professor Zhunian Wang and Professor Jiashui Wang from the Tropical Crop Genetic Resources Institute, Chinese Academy of Tropical Agricultural Sciences (CATAS), for their identification of the *Aloe vera* variety used in this study. The referenced public herbarium is the Chinese Virtual Herbarium, affiliated with the Institute of Botany, Chinese Academy of Sciences. The voucher specimen number is IBSC 0620681.

Author Contributions

All authors made a significant contribution to the work reported, whether that is in the conception, study design, execution, acquisition of data, analysis and interpretation, or in all these areas; took part in drafting, revising or critically reviewing the article; gave final approval of the version to be published; have agreed on the journal to which the article has been submitted; and agree to be accountable for all aspects of the work.

Funding

This research received funding from the National Natural Science Foundation of China [82003379], the Postgraduate Research & Practice Innovation Program of Jiangsu Province [KYCX23_3767], the Zhenjiang Key Laboratory of High Technology Research on Exosomes Foundation and Transformation Application [SS2018003], the Priority Academic

Program Development of Jiangsu Higher Education Institutions [Phase IV, Clinical Medicine], the Open Project of Jiangsu Provincial Key Laboratory of Laboratory Medicine [JSKLM-Z-2024-002], and the Changzhou High-Level Medical Talents Training Project [2022CZBJ105].

Disclosure

The authors report that there are no conflicts of interest in this work.

References

1. Li C, Fu Y, Dai H, Wang Q, Gao R, Zhang Y. Recent progress in preventive effect of collagen peptides on photoaging skin and action mechanism. *Food Sci Hum Wellness*. 2022;11(2):218–229.
2. Rittie L, Fisher GJ. Natural and sun-induced aging of human skin. *Cold Spring Harb Perspect Med*. 2015;5(1):a015370. doi:10.1101/cshperspect.a015370
3. Saric S, Sivamani RK. Polyphenols and Sunburn. *Int J Mol Sci*. 2016;17(9). doi:10.3390/ijms17091521
4. Gilchrest BA. Photoaging. *J Invest Dermatol*. 2013;133(E1):E2–6. doi:10.1038/skinbio.2013.176
5. Liu W, Yan F, Xu Z, et al. Urolithin A protects human dermal fibroblasts from UVA-induced photoaging through NRF2 activation and mitophagy. *J Photochem Photobiol B*. 2022;232:112462.
6. Zhang H, Xiao X, Wang L, et al. Human adipose and umbilical cord mesenchymal stem cell-derived extracellular vesicles mitigate photoaging via TIMP1/Notch1. *Signal Transduct Target Ther*. 2024;9(1):294. doi:10.1038/s41392-024-01993-z
7. Ma J, Teng Y, Huang Y, Tao X, Fan Y. Autophagy plays an essential role in ultraviolet radiation-driven skin photoaging. *Front Pharmacol*. 2022;13:864331. doi:10.3389/fphar.2022.864331
8. Schuch AP, Moreno NC, Schuch NJ, Menck CFM, Garcia CCM. Sunlight damage to cellular DNA: focus on oxidatively generated lesions. *Free Radic Biol Med*. 2017;107:110–124.
9. Pourang A, Tisack A, Ezekwe N, et al. Effects of visible light on mechanisms of skin photoaging. *Photodermatol Photoimmunol Photomed*. 2022;38(3):191–196. doi:10.1111/phpp.12736
10. Sinikumpu SP, Jokelainen J, Haarala AK, Keranen MH, Keinanen-Kiukaanniemi S, Huilaja L. The high prevalence of skin diseases in adults aged 70 and older. *J Am Geriatr Soc*. 2020;68(11):2565–2571. doi:10.1111/jgs.16706
11. Serra D, Garroni G, Cruciani S, et al. Electrospun nanofibers encapsulated with natural products: a novel strategy to counteract skin aging. *Int J Mol Sci*. 2024;25(3):1908. doi:10.3390/ijms25031908
12. Bhatia E, Kumari D, Sharma S, Ahamad N, Banerjee R. Nanoparticle platforms for dermal antiaging technologies: insights in cellular and molecular mechanisms. *Wiley Interdiscip Rev Nanomed Nanobiotechnol*. 2022;14(2):e1746. doi:10.1002/wnan.1746
13. Pinedo M, de la Canal L, de Marcos Lousa C. A call for Rigor and standardization in plant extracellular vesicle research. *J Extracell Vesicles*. 2021;10(6):e12048. doi:10.1002/jev2.12048
14. Tu J, Jiang F, Fang J, et al. Anticipation and verification of dendrobium-derived nanovesicles for skin wound healing targets, predicated upon immune infiltration and senescence. *Int J Nanomed*. 2024;19:1629–1644. doi:10.2147/IJN.S438398
15. Lee Y, Jeong DY, Jeun YC, Choe H, Yang S. Preventive and ameliorative effects of potato exosomes on UVB-induced photodamage in keratinocyte HaCaT cells. *Mol Med Rep*. 2023;28(3). doi:10.3892/mmr.2023.13054
16. Feng J, Xiu Q, Huang Y, Troyer Z, Li B, Zheng L. Plant-derived vesicle-like nanoparticles as promising biotherapeutic tools: present and future. *Adv Mater*. 2023;35(24):e2207826. doi:10.1002/adma.202207826
17. Xiao J, Chen S, Chen Y, Su J. The potential health benefits of aloin from genus Aloe. *Phytother Res*. 2022;36(2):873–890. doi:10.1002/ptr.7371
18. Sanchez M, Gonzalez-Burgos E, Iglesias I, Gomez-Serranillos MP. Pharmacological update properties of Aloe vera and its major active constituents. *Molecules*. 2020;25(6). doi:10.3390/molecules25061324
19. Gao Y, Kuok KI, Jin Y, Wang R. Biomedical applications of Aloe vera. *Crit Rev Food Sci Nutr*. 2019;59(sup1):S244–S256. doi:10.1080/10408398.2018.1496320
20. Salehi B, Albayrak S, Antolak H, et al. Aloe genus plants: from farm to food applications and phytopharmacotherapy. *Int J Mol Sci*. 2018;19(9).
21. Pawlowicz K, Ludowicz D, Karazniewicz-Lada M, Wdowiak K, Cielecka-Piontek J. Analysis of the composition of lyophilisates obtained from Aloe arborescens gel of leaves of different ages from controlled crops. *Molecules*. 2021;26(11). doi:10.3390/molecules26113204
22. Pawlowicz K, Paczkowska-Walendowska M, Osmalek T, Cielecka-Piontek J. Towards the preparation of a hydrogel from lyophilisates of the Aloe arborescens aqueous extract. *Pharmaceutics*. 2022;14(7). doi:10.3390/pharmaceutics14071489
23. Wahedi HM, Jeong M, Chae JK, Do SG, Yoon H, Kim SY. Aloesin from Aloe vera accelerates skin wound healing by modulating MAPK/Rho and Smad signaling pathways in vitro and in vivo. *Phytomedicine*. 2017;28:19–26. doi:10.1016/j.phymed.2017.02.005
24. Rodrigues D, Viotto AC, Checchia R, et al. Mechanism of Aloe vera extract protection against UVA: shelter of lysosomal membrane avoids photodamage. *Photochem Photobiol Sci*. 2016;15(3):334–350. doi:10.1039/c5pp00409h
25. Ramirez O, Pomareda F, Olivares B, et al. Aloe vera peel-derived nanovesicles display anti-inflammatory properties and prevent myofibroblast differentiation. *Phytomedicine*. 2024;122:155108. doi:10.1016/j.phymed.2023.155108
26. Choi SH, Eom JY, Kim HJ, et al. Aloe-derived nanovesicles attenuate inflammation and enhance tight junction proteins for acute colitis treatment. *Biomater Sci*. 2023;11(16):5490–5501. doi:10.1039/d3bm00591g
27. Zhou H, Peng K, Wang J, et al. Aloe-derived vesicles enable macrophage reprogramming to regulate the inflammatory immune environment. *Front Bioeng Biotechnol*. 2023;11:1339941. doi:10.3389/fbioe.2023.1339941
28. Kim M, Park JH. Isolation of Aloe saponaria-derived extracellular vesicles and investigation of their potential for chronic wound healing. *Pharmaceutics*. 2022;14(9):1905. doi:10.3390/pharmaceutics14091905
29. Kim MK, Choi YC, Cho SH, Choi JS, Cho YW. The antioxidant effect of small extracellular vesicles derived from Aloe vera peels for wound healing. *Tissue Eng Regen Med*. 2021;18(4):561–571. doi:10.1007/s13770-021-00367-8
30. Zeng L, Wang H, Shi W, et al. Aloe derived nanovesicle as a functional carrier for indocyanine green encapsulation and phototherapy. *J Nanobiotechnology*. 2021;19(1):439. doi:10.1186/s12951-021-01195-7

31. Zhang M, Viennois E, Prasad M, et al. Edible ginger-derived nanoparticles: a novel therapeutic approach for the prevention and treatment of inflammatory bowel disease and colitis-associated cancer. *Biomaterials*. 2016;101:321–340. doi:10.1016/j.biomaterials.2016.06.018
32. Valentino A, Conte R, Bousta D, et al. Extracellular vesicles derived from Opuntia ficus-indica Fruit (OFI-EVs) speed up the normal wound healing processes by modulating cellular responses. *Int J Mol Sci*. 2024;25(13):7103. doi:10.3390/ijms25137103
33. Salminen A, Kaarniranta K, Kauppinen A. Photoaging: UV radiation-induced inflammation and immunosuppression accelerate the aging process in the skin. *Inflamm Res*. 2022;71(7–8):817–831. doi:10.1007/s00011-022-01598-8
34. Sesto A, Navarro M, Burslem F, Jorcano JL. Analysis of the ultraviolet B response in primary human keratinocytes using oligonucleotide microarrays. *Proc Natl Acad Sci U S A*. 2002;99(5):2965–2970. doi:10.1073/pnas.052678999
35. Xue N, Liu Y, Jin J, Ji M, Chen X. Chlorogenic acid prevents UVA-induced skin photoaging through regulating collagen metabolism and apoptosis in human dermal fibroblasts. *Int J Mol Sci*. 2022;23(13):6941. doi:10.3390/ijms23136941
36. Masaki H. Role of antioxidants in the skin: anti-aging effects. *J Dermatol Sci*. 2010;58(2):85–90. doi:10.1016/j.jdermsci.2010.03.003
37. Harman D. The free radical theory of aging. *Antioxid Redox Signal*. 2003;5(5):557–561. doi:10.1089/152308603770310202
38. Gu Y, Han J, Jiang C, Zhang Y. Biomarkers, oxidative stress and autophagy in skin aging. *Ageing Res Rev*. 2020;59:101036. doi:10.1016/j.arr.2020.101036
39. Zhou Y, Liu Y, Gao F, et al. β-Galactosidase: insights into source variability, genetic engineering, immobilisation and diverse applications in food, industry and medicine. *Int J Dairy Technol*. 2024;77(3):651–679. doi:10.1111/1471-0307.13098
40. Xu P, Xin Y, Zhang Z, et al. Extracellular vesicles from adipose-derived stem cells ameliorate ultraviolet B-induced skin photoaging by attenuating reactive oxygen species production and inflammation. *Stem Cell Res Ther*. 2020;11(1):264. doi:10.1186/s13287-020-01777-6
41. Lu F, Zhou Q, Liang M, et al. alpha-Arbutin ameliorates UVA-induced photoaging through regulation of the SIRT3/PGC-1alpha pathway. *Front Pharmacol*. 2024;15:1413530. doi:10.3389/fphar.2024.1413530
42. Perez-Ferriols A. The minimal erythema dose (MED) project: in search of consensus on phototesting. *Actas Dermosifiliogr*. 2013;104(7):541–542. doi:10.1016/j.adengl.2013.04.012
43. Rufini A, Tucci P, Celardo I, Melino G. Senescence and aging: the critical roles of p53. *Oncogene*. 2013;32(43):5129–5143. doi:10.1038/onc.2012.640
44. Hirota A, Kawachi Y, Itoh K, et al. Ultraviolet A irradiation induces NF-E2-related factor 2 activation in dermal fibroblasts: protective role in UVA-induced apoptosis. *J Invest Dermatol*. 2005;124(4):825–832. doi:10.1111/j.0022-202X.2005.23670.x
45. Zhu S, Qin W, Liu T, et al. Modified Qing'e Formula protects against UV-induced skin oxidative damage via the activation of Nrf2/ARE defensive pathway. *Front Pharmacol*. 2022;13:976473. doi:10.3389/fphar.2022.976473
46. Melo CPB, Saito P, Vale DL, et al. Protective effect of oral treatment with Cordia verbenacea extract against UVB irradiation deleterious effects in the skin of hairless mouse. *J Photochem Photobiol B*. 2021;216:112151. doi:10.1016/j.jphotobiol.2021.112151
47. Ding YW, Zhao GJ, Li XL, et al. SIRT1 exerts protective effects against paraquat-induced injury in mouse type II alveolar epithelial cells by deacetylating NRF2 in vitro. *Int J Mol Med*. 2016;37(4):1049–1058. doi:10.3892/ijmm.2016.2503
48. Chaiprasongsuk A, Panich U. Role of phytochemicals in skin photoprotection via regulation of Nrf2. *Front Pharmacol*. 2022;13:823881. doi:10.3389/fphar.2022.823881
49. Ming T, de Richter R, Shen S, Caillol S. Fighting global warming by greenhouse gas removal: destroying atmospheric nitrous oxide thanks to synergies between two breakthrough technologies. *Environ Sci Pollut Res Int*. 2016;23(7):6119–6138. doi:10.1007/s11356-016-6103-9
50. Portmann RW, Daniel JS, Ravishankara AR. Stratospheric ozone depletion due to nitrous oxide: influences of other gases. *Philos Trans R Soc Lond B Biol Sci*. 2012;367(1593):1256–1264. doi:10.1098/rstb.2011.0377
51. Zhou W, Liu W, Zou L, et al. Storage stability and skin permeation of vitamin C liposomes improved by pectin coating. *Colloids Surf B Biointerfaces*. 2014;117:330–337. doi:10.1016/j.colsurfb.2014.02.036
52. Stanly C, Fiume I, Capasso G, Pocsfalvi G. Isolation of exosome-like vesicles from plants by ultracentrifugation on sucrose/deuterium oxide (D2O) density cushions. *Methods Mol Biol*. 2016;1459:259–269.
53. Lian MQ, Chng WH, Liang J, et al. Plant-derived extracellular vesicles: recent advancements and current challenges on their use for biomedical applications. *J Extracell Vesicles*. 2022;11(12):e12283. doi:10.1002/jev2.12283
54. Solaberrieta I, Jimenez A, Garrigos MC. Valorization of Aloe vera skin by-products to obtain bioactive compounds by microwave-assisted extraction: antioxidant activity and chemical composition. *Antioxidants*. 2022;11(6).
55. Zhang Y, Bao Z, Ye X, et al. Chemical investigation of major constituents in Aloe vera leaves and several commercial Aloe juice powders. *J AOAC Int*. 2018;101(6):1741–1751.
56. Wu P, Zhang B, Han X, et al. HucMSC exosome-delivered 14-3-3zeta alleviates ultraviolet radiation-induced photodamage via SIRT1 pathway modulation. *Aging*. 2021;13(8):11542–11563. doi:10.18632/aging.202851
57. Picca A, Faitg J, Auwerx J, Ferrucci L, D'Amico D. Mitophagy in human health, ageing and disease. *Nat Metab*. 2023;5(12):2047–2061. doi:10.1038/s42255-023-00930-8